The enigmatic iron oxyhydroxysulfate nanomineral schwertmannite: Morphology, structure, and composition

Rebecca A. French[1,2*], Manuel A. Caraballo[3], Bojeong Kim[1,2], J.D. Rimstidt[2], Mitsuhiro Murayama[4,5], Michael F. Hochella Jr.[1,2]

[1]Environmental Nanoscience and Technology Laboratory, ICTAS, Virginia Tech, Blacksburg, VA 24061, U.S.A.

[2]Department of Geosciences, Virginia Tech, Blacksburg, VA 24061, U.S.A.

[3]Geology Department, University of Huelva, Campus "El Carmen", E-21071 Huelva, Spain

[4]Nanoscale Characterization and Fabrication Laboratory, ICTAS, Virginia Tech, Blacksburg, VA 24061, U.S.A.

[5]Department of Materials Science and Engineering, Virginia Tech, Blacksburg, VA 24061, U.S.A.

*E-mail address: rafrench@vt.edu

Supplemental Information

Table of Contents

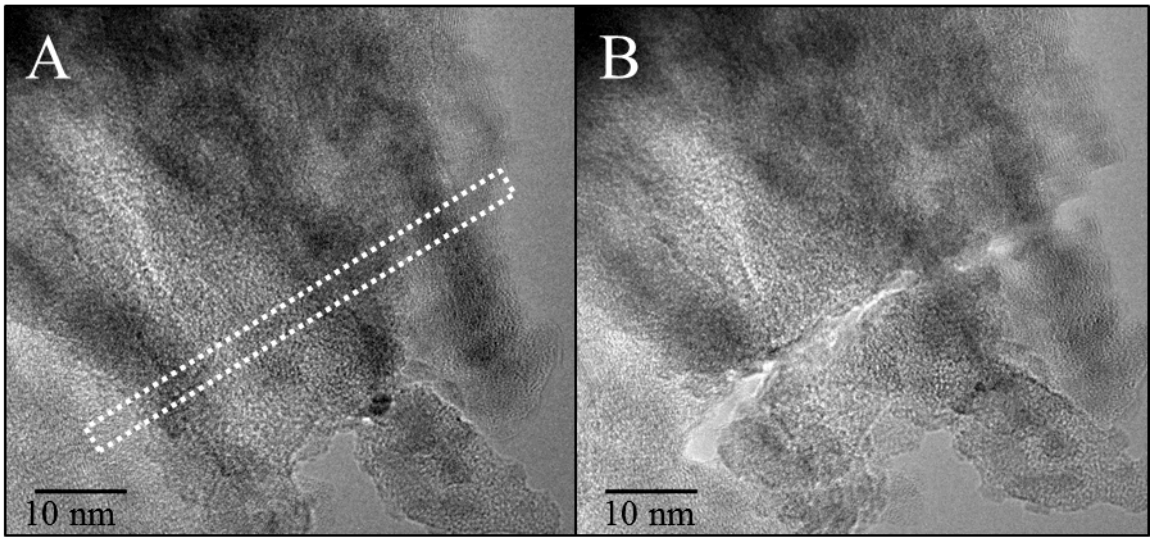

Figure S1. (A) TEM image of a needle on the surface of a schwertmannite particle from the TSR site. The white dotted rectangle indicates the area over which EDX analyses were performed across a portion of this needle. (B) TEM image of the same area as (A) after EDX analyses have been completed within the white dotted region in (A). Sample degradation is clearly observed. In this study, HRTEM was always completed before EDX analyses were performed.

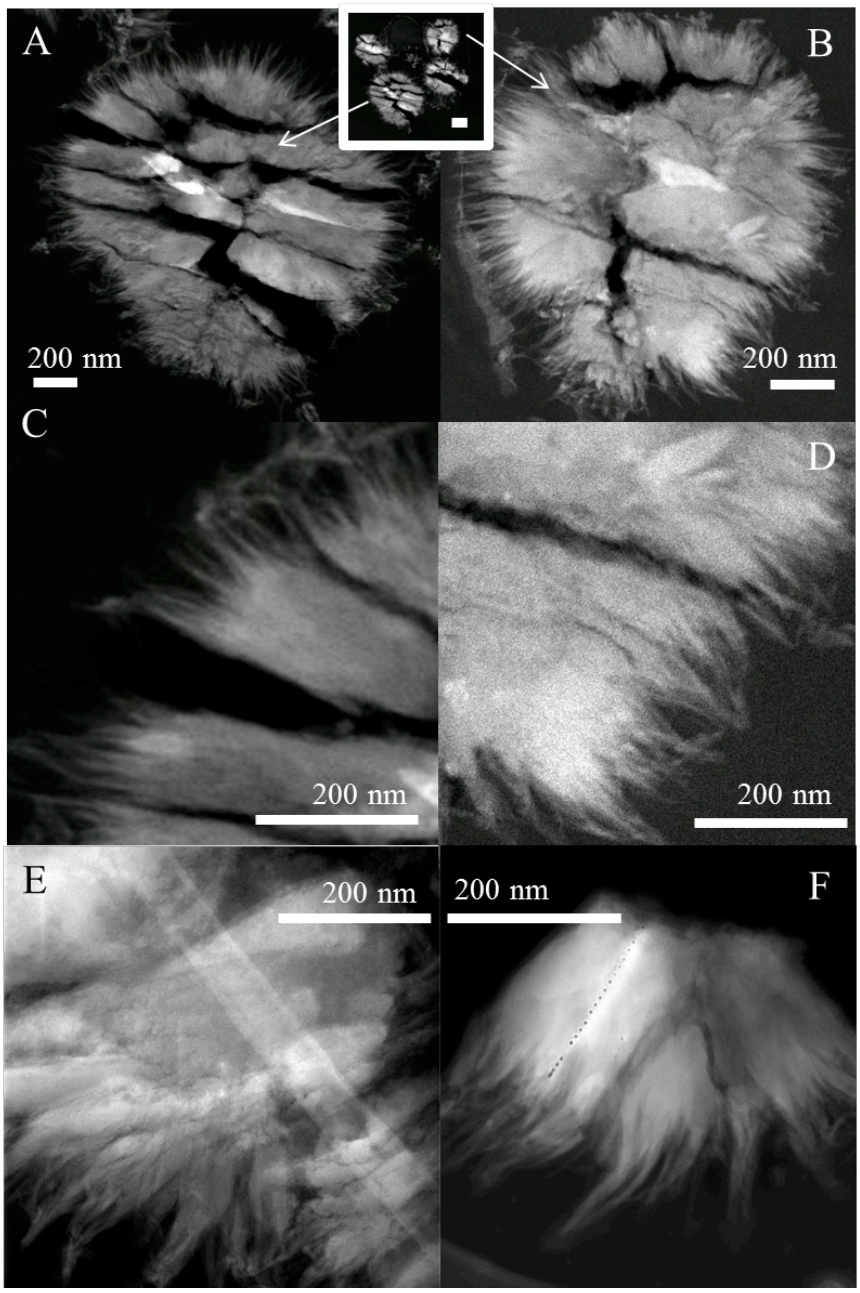

Figure S2. All of the above HAADF TEM images show ultramicrotomed thin sections of schwertmannite from the MR site. The scale bar for the inset between (A) and (B) is 500 nm. (C) and (D) show magnified areas of portions of (A) and (B), respectively. (E) and (F) show thin sections of schwertmannite samples collected in the TSR site. We believe that the cracks across the schwertmannite thin sections – seen in (A) and (B) – result from the cutting process because these types of cracks were characteristic of all schwertmannite particles that were ultramicrotomed and were all in the same orientation. No evidence for these types of cracks was ever seen when imaging the schwertmannite particles as whole aggregates. (F) shows a portion of a schwertmannite particle that was broken during the cutting process. The small holes that are visible on the left side of the section were created during EDX data collection.

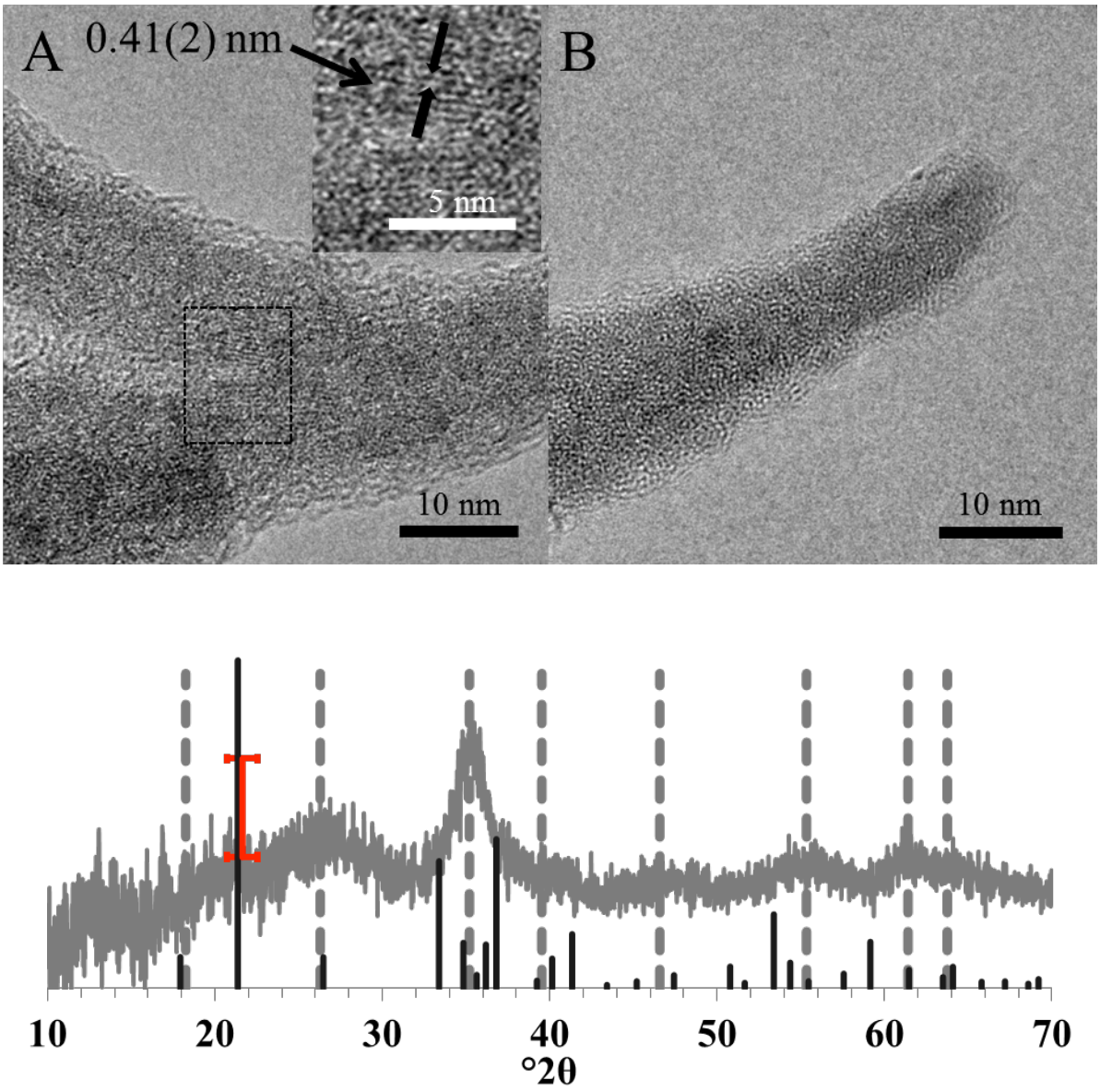

Figure S3. The images are from a needle on the surface of a schwertmannite particle collected at the TSR site (same as Figure 4, main text). The powder XRD pattern for the bulk TSR schwertmannite is also shown. The grey dashed vertical lines show the position of the broad peaks of the schwertmannite XRD pattern (Cornell and Schwertmann, 2003), and the black vertical lines represent the position and intensity of peaks from the goethite XRD pattern. The location of the d-spacing measured from the lattice fringes in image (A) is marked (red line with horizontal error bars calculated as the standard deviation of multiple measurements of the lattice fringes). This d-spacing matches well with the (101) peak in the goethite XRD pattern.

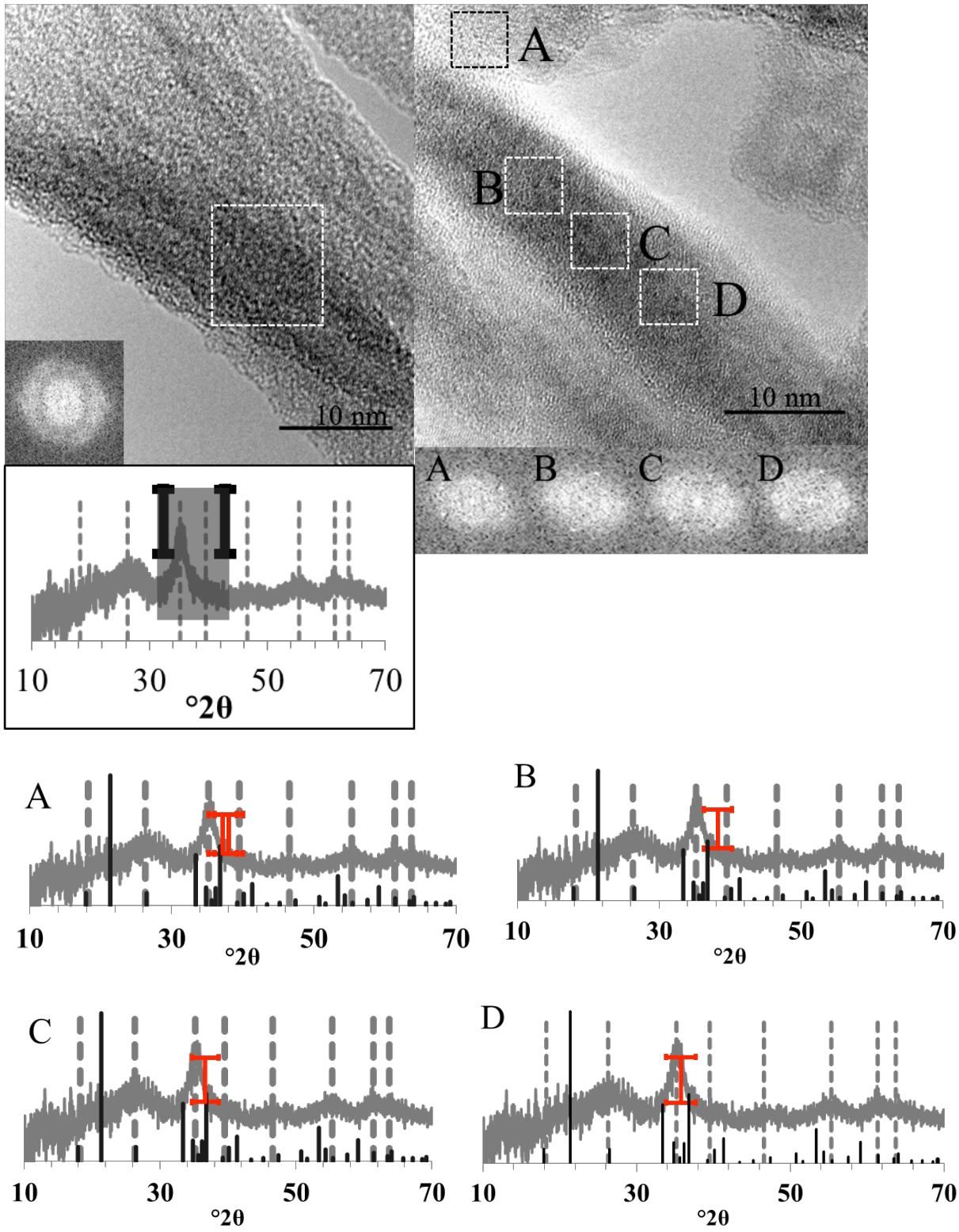

Figure S4. Text accompanying Figure 5 in the main article explains the left image and the diffraction pattern just below it. The right image is also shown in Figure 5 in the main article, but the FFT patterns are described here, with the addition of the MR schwertmannite XRD patterns below. The d-spacings calculated from the FFT patterns labeled A-D, from the

corresponding areas of the right image, are shown in the XRD patterns in red. The error bars (horizontal, red) were calculated based on the method described below. The black lines on the horizontal axis of these XRD patterns are the goethite standard d-spacings and the grey dotted lines are the schwertmannite literature values (Cornell and Schwertmann, 2003).

The error bars on the d-spacings marked in red are calculated based on the pixel size of the FFT spectra of the HRTEM images. The d-spacings were measured by converting the number of pixels from an FFT image to the equivalent distance in nanometers. These types of measurements are limited by the pixel size of the image. The error in our measurements is the °2θ equivalent of plus or minus 1 pixel length of the measured d-spacing in pixels. For example, if we measured the distance between the center of an FFT spot pattern and a spot to be 35 pixels and 1 pixel = 0.18 nm^{-1}, then the d-spacing (d) would be

$$d = \frac{1}{35 \times 0.18} \quad (1)$$

and the d-spacing measured, if the actual length was plus one pixel would be

$$d = \frac{1}{36 \times 0.18} \quad (2)$$

and similarly, the d-spacing for minus one pixel would be

$$d = \frac{1}{34 \times 0.18} \quad (3)$$

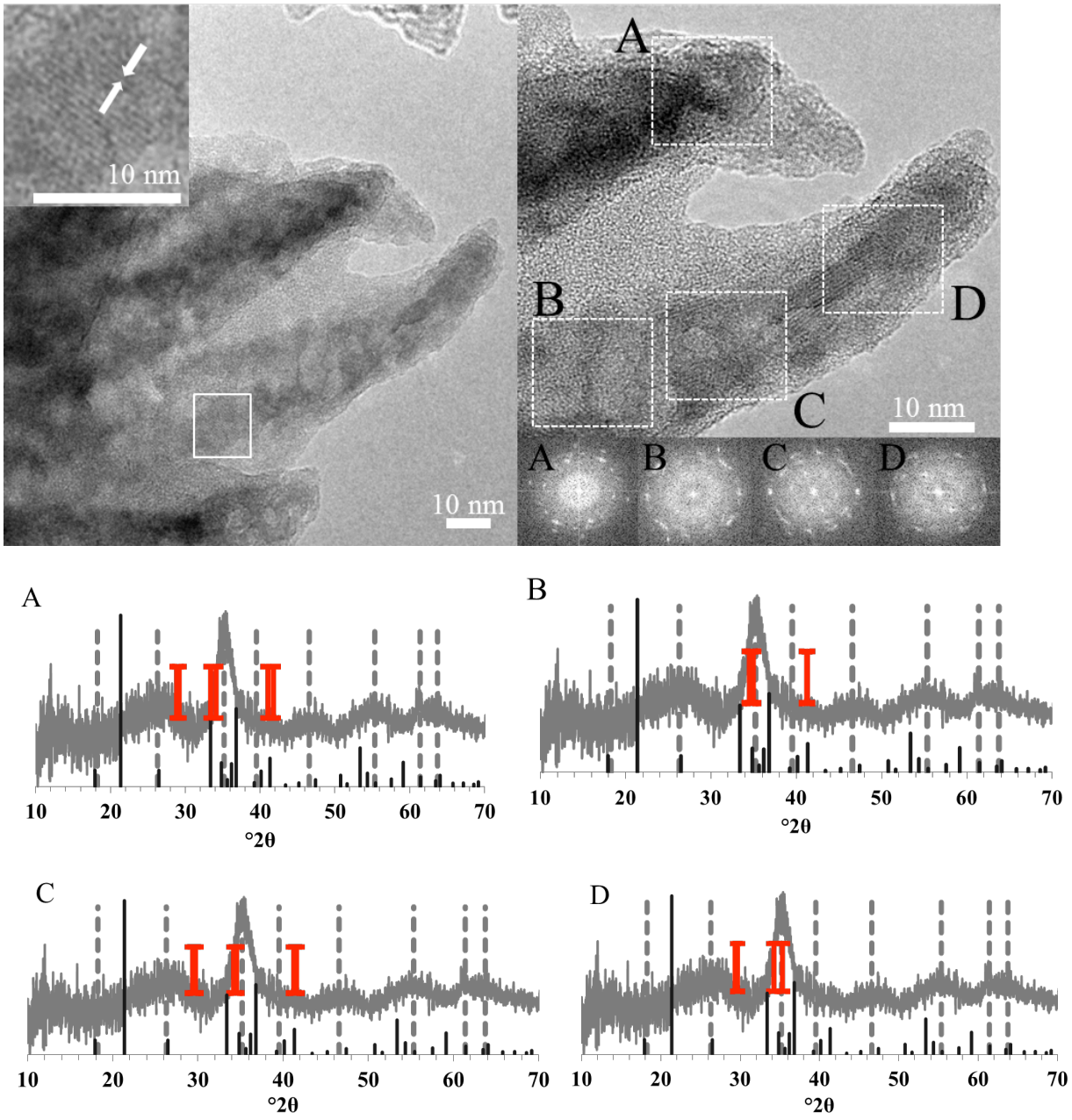

Figure S5. The images and FFT patterns here are the same as Figure 6 in the main article, but the TSR schwertmannite XRD patterns below have been added and are explained here. The d-spacings calculated from the FFT patterns labeled A-D, from the corresponding areas of the image, are shown in the XRD patterns in red. The error bars (horizontal, red) were calculated based on the method described in Figure S4. The black lines on the horizontal axis of these XRD patterns are the goethite standard d-spacings and the grey dotted lines are the schwertmannite literature values (Cornell and Schwertmann, 2003).

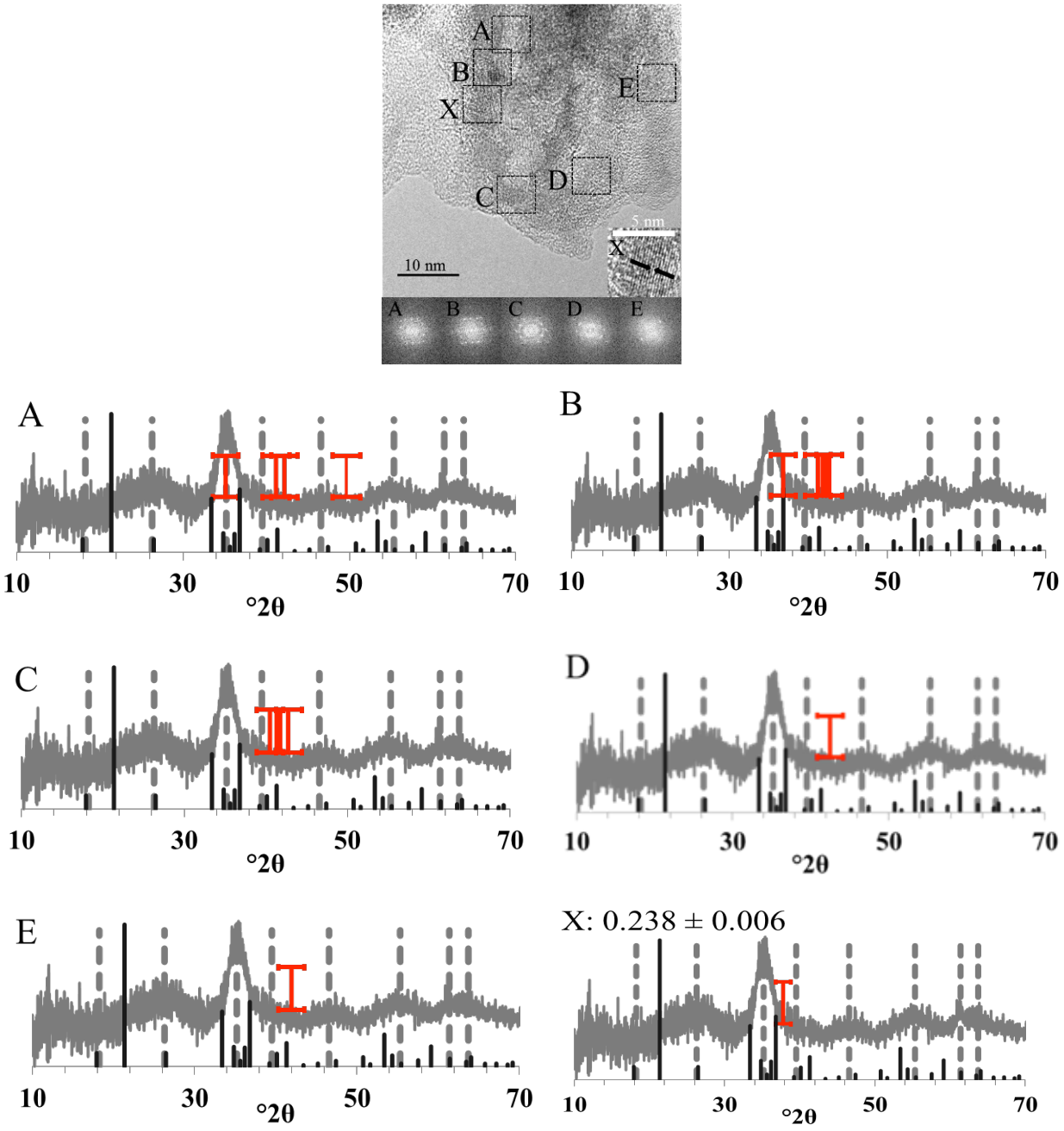

Figure S6. The TEM image and FFT patterns here are the same as Figure 7 in the main article, but the TSR schwertmannite XRD patterns below have been added and are explained here. The d-spacings calculated from the FFT patterns labeled A-E, from the corresponding areas of the image, are shown in the XRD patterns in red. The error bars (horizontal, red) for A-E were calculated based on the method described in Figure S4. The d-spacing for area X (0.238 nm) is also shown in red with error bars, but the error bars were calculated as the standard deviation (0.006 nm) of multiple measurements of the lattice fringes. The black lines on the horizontal axis of these XRD patterns are the goethite standard d-spacings and the grey dotted lines are the schwertmannite literature values (Cornell and Schwertmann, 2003).

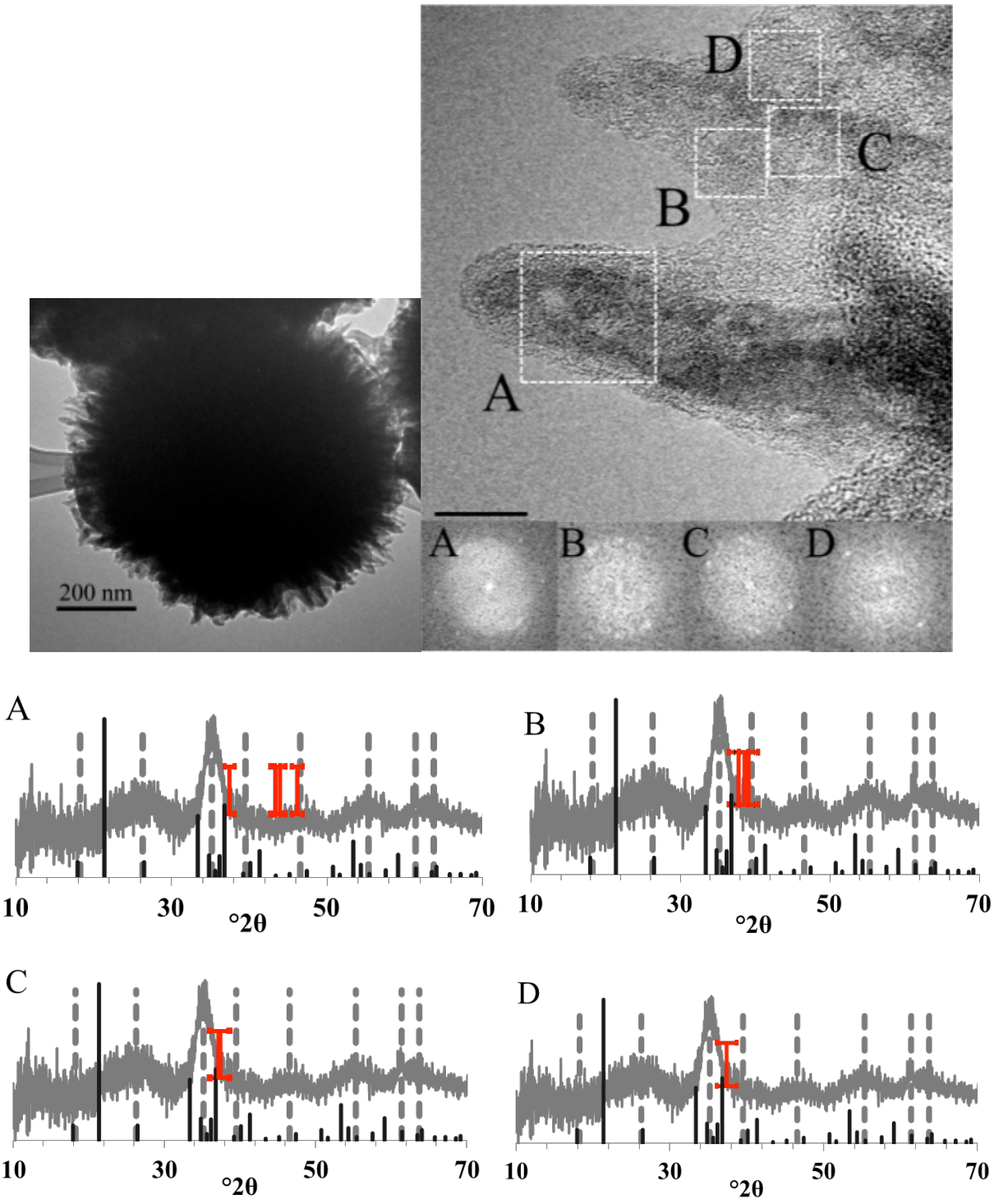

Image area	Schwertmannite XRD peak (nm)	Goethite plane
A,B,C,D	0.255	A,B,C,D (111); C,D: (400)
B	0.228	(002) (211)
A	0.195	(202) (311)

Figure S7. Left TEM image is a schwertmannite particle from the TSR mine and the right TEM image shows needles from the surface of that same schwertmannite particle. Insets in the right

image show the FFT patterns of the corresponding areas (white boxes) in the TEM image. The d-spacings measured from the FFT analyses are shown in red on the TSR schwertmannite XRD patterns. The error bars (horizontal, red) for the measured d-spacings were calculated based on the method described in Figure S4. The grey dashed vertical lines show the position of the broad peaks of the schwertmannite XRD pattern (Cornell and Schwertmann, 2003), and the black vertical lines represent the position and intensity of peaks from the goethite XRD pattern. The table gives the schwertmannite peak and goethite planes that align with the measured d-spacings for each image area. For example, images A,B,C, and D all have a d-spacing that aligns with the 0.255 nm schwertmannite peak and the (111) goethite plane.

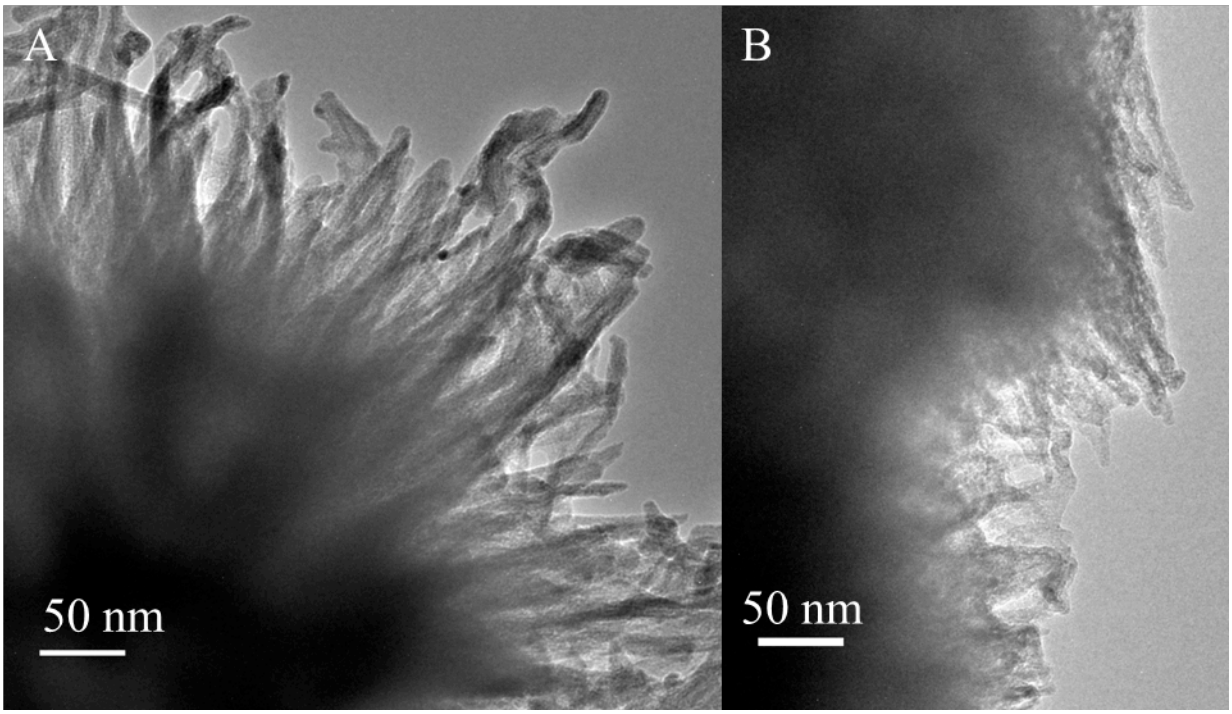

Figure S8. Lower magnification views of schwertmannite particles whose needles were used for structural analysis using FFT of HRTEM images. (A) MR schwertmannite particle area from which images for Figure 5 and 8 and supplemental Figure S9 were taken. (B) TSR schwertmannite particle area from which images for Figure 9 and supplemental Figures S10 and S13 were taken.

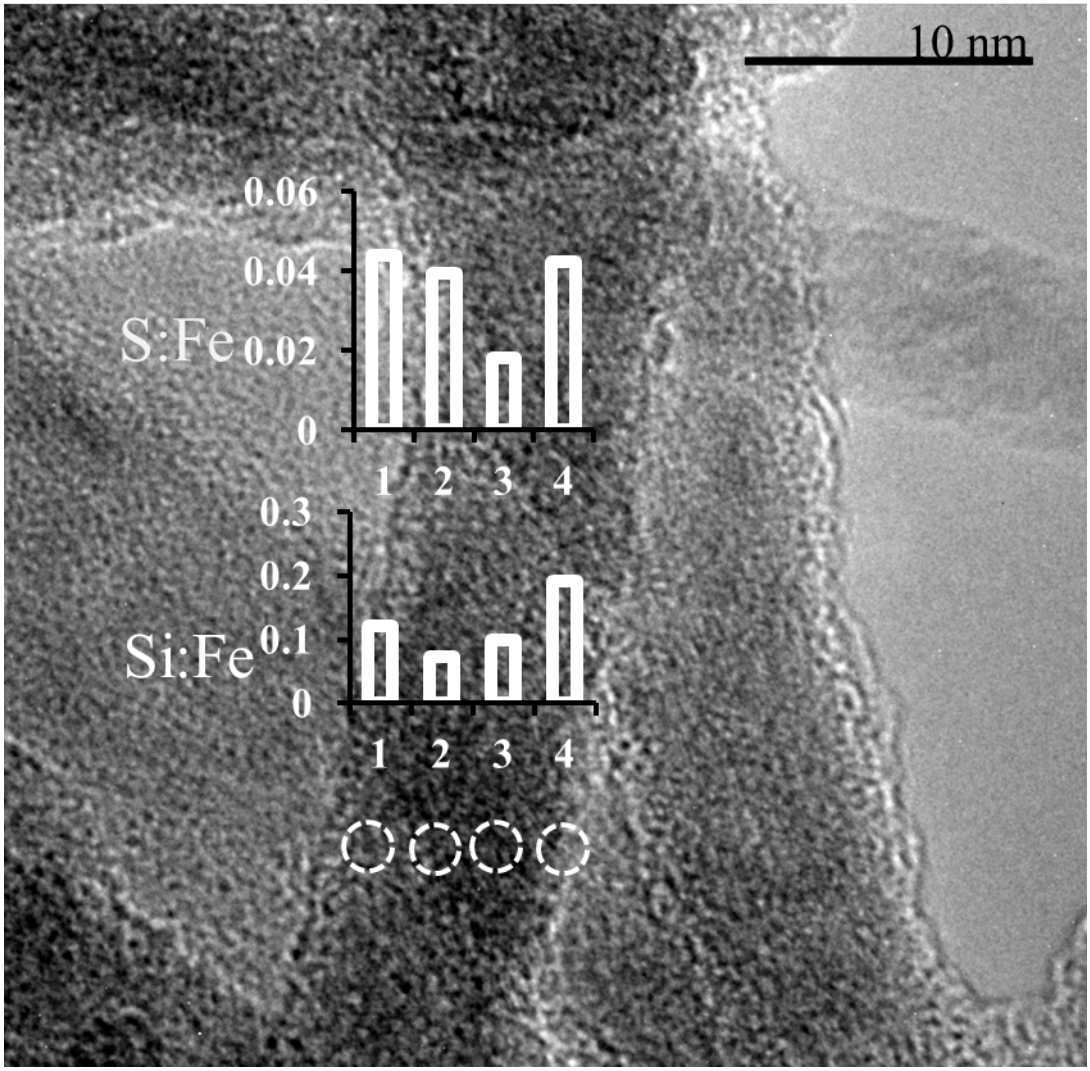

Figure S9. The TEM image shows needles from a schwertmannite particle from the MR site. The bar graphs show S:Fe and Si:Fe ratios calculated from integrated peak intensity of EDX data collected at 4 points, whose approximate location is shown by the white dashed circles.

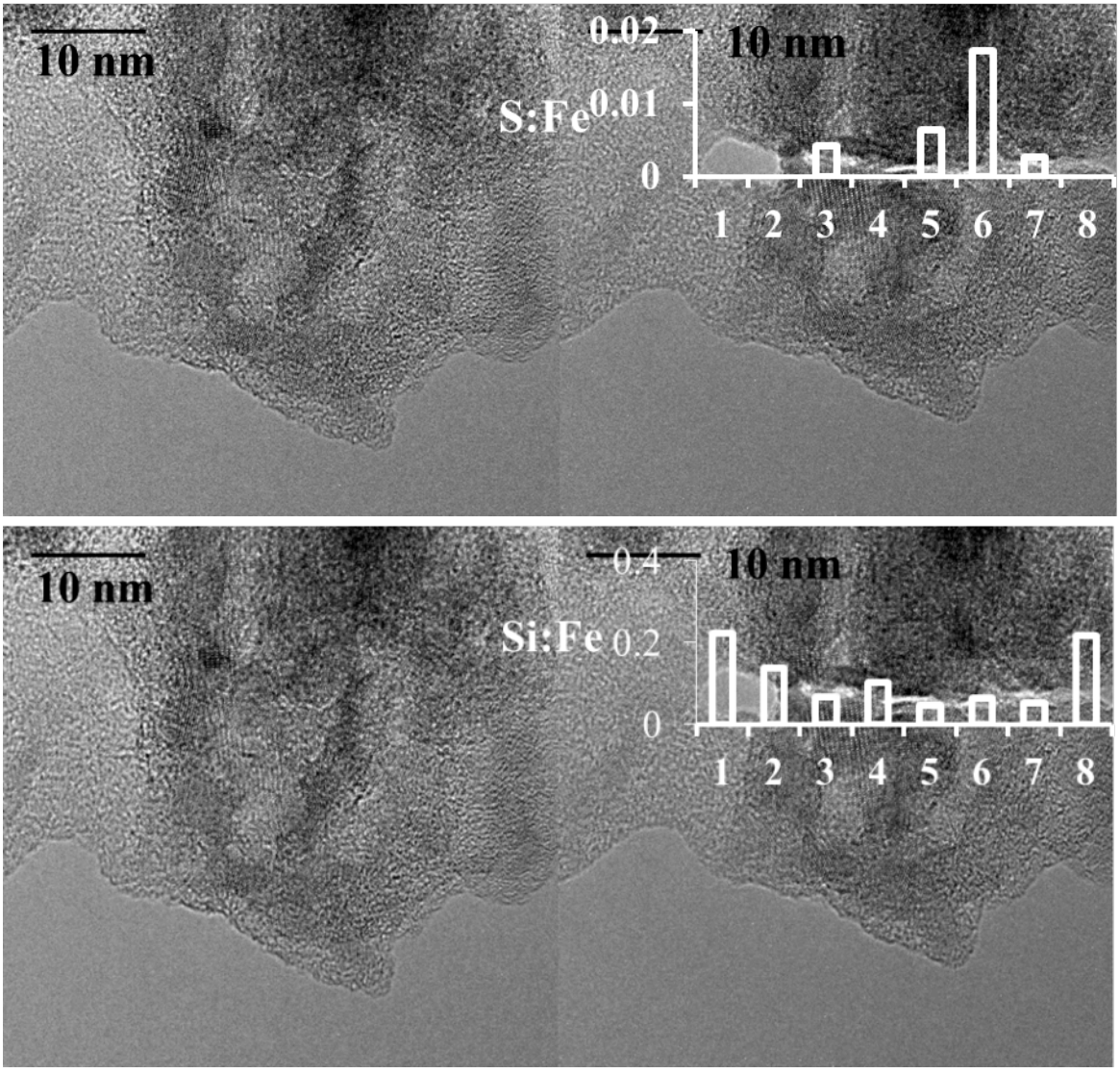

Figure S10. The TEM images above show schwertmannite needles from the TSR site. Images on the left are pre-EDX analysis. The holes in the images on the right are where the EDX analyses were performed. The sample was locally severely degraded during EDX analysis. The area between the ticks on the x-axis of the bar graph gives the approximate location where one EDX sampling area ends and the next sampling area begins within the area that was degraded during sample collection. S:Fe and Si:Fe ratios, calculated from integrated peak intensity of EDX data, are shown in the bar graph in the images on the right. The chemical information in the graph can be read as a description of the composition of the schwertmannite needle material that previously existed before the sample was degraded during sample analysis.

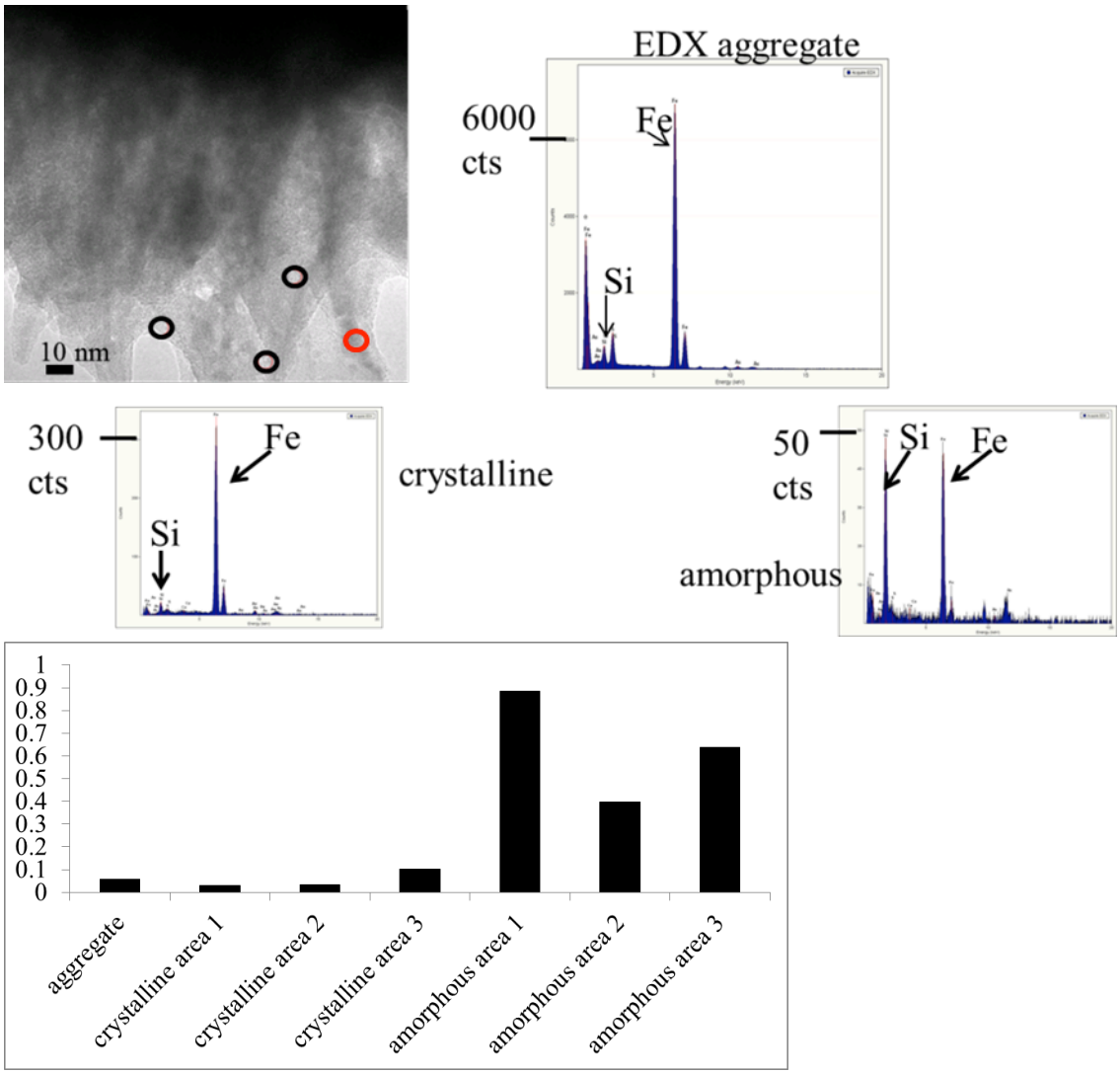

Figure S11. The bar graph above shows a semi-quantitative comparison of the average Si:Fe ratio of an entire schwertmannite 'aggregate' (TEM image of aggregate shown in the Figure 3B main article) relative to the Si:Fe ratios in ~ 5 nm spot size areas within the needles of that same aggregate (TEM image above). An example EDX spectrum of an entire schwertmannite aggregate, labeled "EDX aggregate," is shown above. The black circles on the TEM image above indicate the 'amorphous' areas where EDX data was collected. EDX data on three 'crystalline' areas was similarly collected in the same field of view as the image above and using the same electron beam spot size that was used in the 'amorphous' area data collection. Crystalline areas were defined by the presence of visible lattice fringes and darker contrast. For example, the red circle shows an area that would have been considered crystalline by these standards. Example EDX spectra for the crystalline and amorphous areas are also shown above. Si:Fe ratios are calculated from the intensity ratio of the integrated area of the K-peak for Si relative to the K-peak for Fe. These ratios should not be interpreted as absolute concentrations of silicon or iron (see text in the main article for explanation).

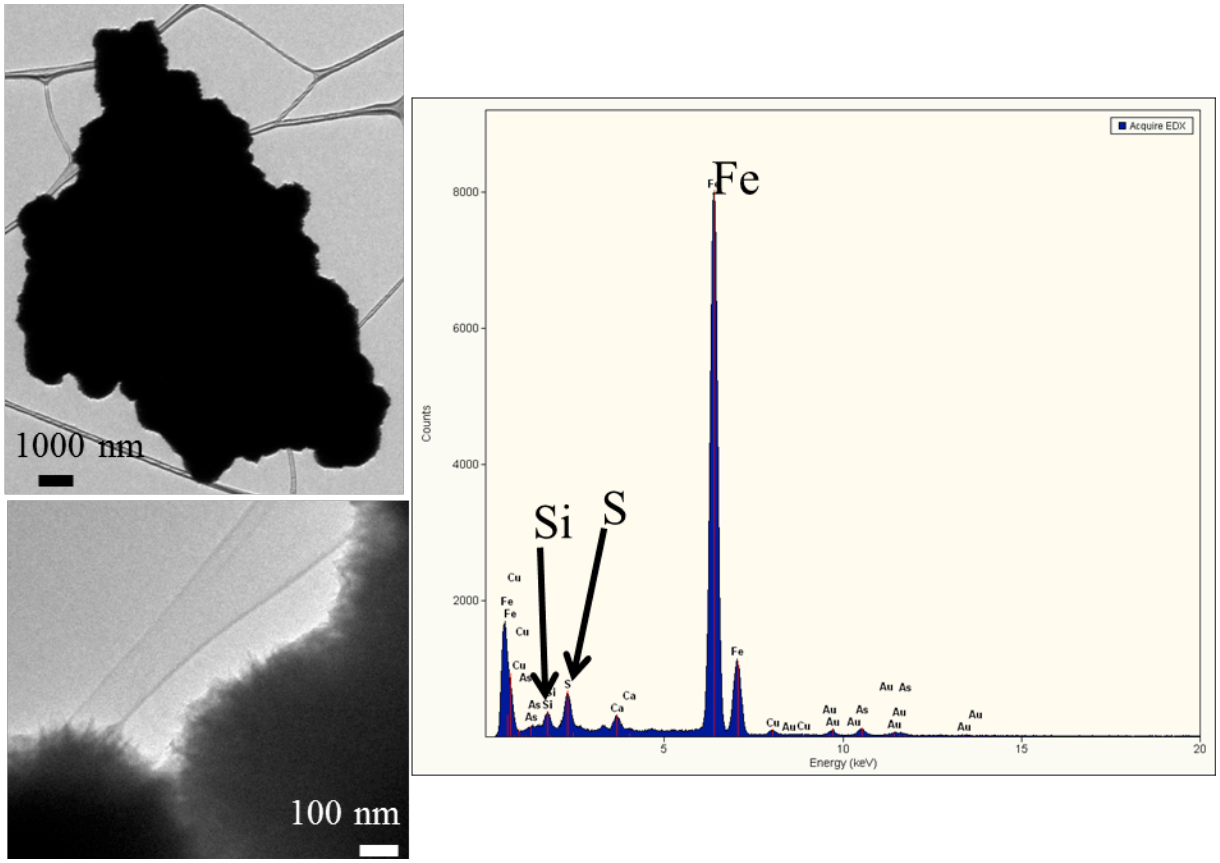

Figure S12. This figure shows another schwertmannite aggregate from the TSR site not seen in other figures in this paper. The EDX data (graph right) collected on the entire aggregate (TEM image upper left) demonstrates that the low Si:Fe ratio, observed in the aggregate in Figure S11, was also seen in the schwertmannite aggregate shown here. The TEM image in the lower left shows individual schwertmannite particles from the larger aggregate (upper left). These particles exhibit the typical TSR schwertmannite morphology (see main text for a description of this morphology).

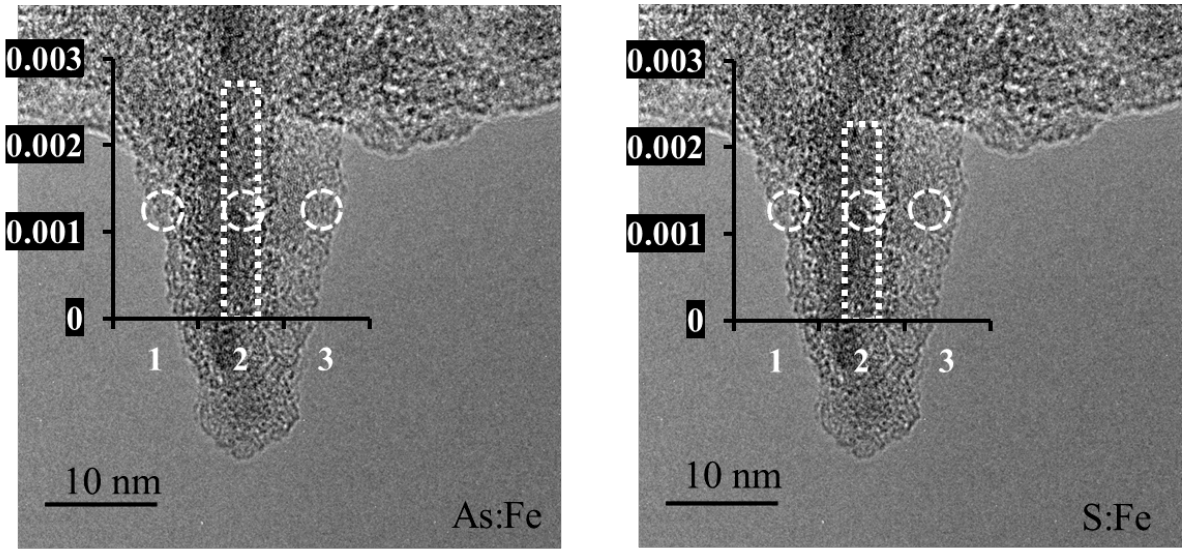

Figure S13. The TEM images above show the distribution of arsenic and sulfur in a needle of schwertmannite from the TSR site. The approximate location of the EDX sampling area is shown by the white circles. Ratios of As:Fe and S:Fe are shown in the bar graph. There is no data for sampling points 1 and 3 because there was no As or S detected in these areas. The ratios of As:Fe and S:Fe should not be directly compared to each other (see text in main article for explanation).

Reference

Cornell, R.M., and Schwertmann, U. (2003) The Iron Oxides. 664 p. Wiley-VCH, Weinheim.